


PET/TPU nanofiber composite filters with high interfacial adhesion strength based on one-step co-electrospinning

Journal Article**Author(s):**

Guo, Yinghe; Guo, Yuchen; He, Weidong; Zhao, Yi-Bo; Shen, Ruiqing; Liu, Jingxian; [Wang, Jing](#) 

Publication date:

2021-07

Permanent link:

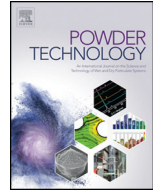
<https://doi.org/10.3929/ethz-b-000479925>

Rights / license:

[Creative Commons Attribution 4.0 International](#)

Originally published in:

Powder Technology 387, <https://doi.org/10.1016/j.powtec.2021.04.020>



PET/TPU nanofiber composite filters with high interfacial adhesion strength based on one-step co-electrospinning

Yinghe Guo^{a,b,c}, Yuchen Guo^{a,d}, Weidong He^{a,b,c}, Yibo Zhao^{b,c}, Ruiqing Shen^e, Jingxian Liu^{a,**}, Jing Wang^{b,c,*}

^a Filter Test Center, Northeastern University, Shenyang, Liaoning 110819, China

^b Institute of Environmental Engineering, ETH Zürich, CH-8093, Switzerland

^c Lab of Advanced Analytical Technologies, EMPA, Dübendorf CH-8600, Switzerland

^d Jilin University of Architecture and Technology, Changchun, Jilin 130114, China

^e Artie McFerrin Department of Chemical Engineering, Texas A&M University, College Station, TX 77843-3122, USA

ARTICLE INFO

Article history:

Received 4 November 2020

Received in revised form 8 March 2021

Accepted 8 April 2021

Available online 10 April 2021

Keywords:

Nanofiber filter media

Co-electrospinning

One-step fabrication

Adhesion strength

Filtration performance

ABSTRACT

Nanofiber membranes are widely employed to prepare composite filter media. The traditional composite method of hot pressing may damage the structure of nanofiber membrane, and thus increase the pressure drop through the composite filter. In this study, three-dimensional PET/TPU (polyethylene terephthalate/thermoplastic polyurethane) composite nanofiber filters (PET/TPU-CNF) with beads-on-string structure were fabricated by one-step co-electrospinning. Besides a stronger adhesion strength of 1.385 N/cm between the nanofiber membrane and substrate, the PET/TPU-CNF presented a low pressure drop of 28.96 Pa and a filtration efficiency of 83.64% for ambient particles at a face velocity of 5.3 cm/s. A high tensile strength of 4.33 MPa was measured for the PET/TPU nanofiber membrane. Thanks to the beads-on-string structure, both the mechanical properties and filtration performances of PET/TPU-CNF were enhanced compared with the pure PET nanofiber composite filter. The present study provides a new route to improve the membrane adhesion strength of nanofiber membrane coated filters.

© 2021 The Author(s). Published by Elsevier B.V. This is an open access article under the CC BY license (<http://creativecommons.org/licenses/by/4.0/>).

1. Introduction

PM_{2.5}, which is defined as the particulate matter with a size less than 2.5 μm, has caused serious concerns in recent years because of its threat to public health [1]. Owing to the small particle size, PM_{2.5} is hard to be captured by the nasal hair [2] and can penetrate human bronchi and deposit in the lung [3], which causes an increased risk of respiratory diseases. Fibrous filters are widely used to control particle pollution. Nowadays, nanofiber media have emerged as a class of promising media which can provide a greater filtration efficiency for the fine particles than conventional microfibers [4]. Electrospinning is a general method used to fabricate nanofiber membrane [5]. Many nanofiber membranes, such as polyacrylonitrile (PAN) [6], poly(vinylidene fluoride) (PVDF) [7], polyvinyl chloride [8], polyimide [9], and polyamide-66 (PA-66) [10], have been successfully prepared by electrospinning. However, these nanofiber membranes could not be used independently because of the soft and fragile structure [11]. In the air filtration field, the

coarse filter substrate (abbreviate as substrate) with certain rigidity is usually employed as the supporting layer for nanofiber membrane coated filter media [12]. However, the weak interfacial adhesion between the nanofiber membrane and substrate reduces the reliability of the composite filter media during long term use [13]. The detachment of nanofiber membrane from the substrate due to the deficient interfacial adhesion may degrade the filtration performance of filter media and further cause the ineffectiveness of the overall filtration system [14,15]. Thus, it is necessary to investigate the membrane composite method to enhance the interfacial adhesion between the nanofiber membrane and the substrate.

Hot pressing, which relies on various adhesives, is a common method for producing membrane coated air filters [16,17]. Among the adhesives of different phases, the liquid and pasty adhesives significantly increase the pressure drop by clogging the pores of both the nanofiber membrane and the substrate. In comparison, the solid adhesives have fewer effects on the pressure drop. Polyvinyl acetate (PVA), polyamides, and thermoplastic polyurethane (TPU) are three typical solid thermoplastic adhesives used in the composite fabrication of paper, board, textile, ceramics, and foils [18–20]. The mechanical performance of PVA is poor in wet or high temperature conditions [21], and the hot press temperature (215–260 °C) of polyamides is higher than the melting temperatures of most supporting coarse filter substrate,

* Corresponding author at: Institute of Environmental Engineering, ETH Zürich, CH-8093, Switzerland.

** Corresponding author at: Filter Test Center, Northeastern University, Shenyang, Liaoning 110819, China.

E-mail addresses: 82003@126.com (J. Liu), jing.wang@ifu.baug.ethz.ch (J. Wang).

e.g. polypropylene (PP) nonwoven (160 °C) and polyethylene terephthalate (PET) (250–255 °C). Therefore, PVA and polyamides are rarely used as adhesives in the membranes coated air filter media. TPU has a lower melting point and better chemical resistance compared with PVA and polyamides. Thus, it has been used as an adhesive in various fields [22]. To avoid the damage of filter substrate, TPU film was used as the adhesive in hot pressing to prepare membrane coated filter media [23]. However, the breakage of nanofiber membrane structure induced by the pressure and high temperature is inevitable, which results in the nanofiber membrane with a lower porosity [24,25]. It is well known that the porosity reduction of filter media will cause an increase in pressure drop and induce a worse filtration performance. Therefore, a proper fabrication method of composite filters should not only provide enough interfacial adhesion, but also maintain the mechanical structure of the nanofiber membrane and supporting substrate. So far, few studies of nanofiber membrane coated filter media have been conducted on the interfacial adhesion strength between the nanofiber membrane and the substrate in the open literature.

In the present study, three-dimensional PET/TPU composite nanofiber filters (PET/TPU-CNF) were fabricated by embedding TPU fibers with beads into nanofiber membrane via one-step co-electrospinning. A commercial filter paper was used as the supporting substrate. The PET nanofibers and the TPU fibers with beads were co-electrospun by setting the temperature of PET and TPU solutions to room temperature and 105 °C, respectively. The morphology, mechanical property, adhesion strength, and filtration performance of the PET/TPU-CNF were tested to evaluate the coating method based on one-step co-electrospinning. The results demonstrated that the PET/TPU-CNF showed high filtration efficiencies for ambient particles and nanoscale particles. Compared with the composite filter consisting of pure PET nanofiber and substrate (PET-CNF), the tensile strength of the PET/TPU nanofiber membrane and the adhesion strength between the PET/TPU nanofiber membrane and substrate were significantly enhanced. Compared with the hot pressing process, no damage to the nanofiber membrane occurred during the composite procedure in the present study. In the PET/TPU-CNF, the melting TPU fibers with beads contributed to the enhancement of the interfacial adhesion between the PET/TPU nanofiber membrane and the substrate, as well as the interlayer adhesion of the PET/TPU nanofiber membrane. This work provides a new route to improve the membrane adhesion strength of nanofiber membrane coated filter media.

2. Materials and methods

2.1. Materials

Polyethylene terephthalate (PET) used in this study was purchased from Shanghai Yuanfang company. Thermoplastic polyurethanes (TPU) was purchased from Dongguan Youxin Plastic Co., Ltd., China. The solvents, trifluoroacetic acid (TFA, C·P) and dichloromethane (DCM, A.R), were of analytical grade and supplied by Jinan Xinshidai Chemical Co., Ltd. and Tianjin Fuyu Chemical Co., Ltd., respectively. *N,N*-dimethylformamide (DMF, A.R) and Tetrahydrofuran (THF, A.R) were purchased from Shanghai Chemical Reagents Co., Ltd., China. The substrate was PET filter paper consisting of PET microfibers (Fig. S1a), which was supplied by Nanjing Meiai Co., Ltd., China.

2.2. Fabrication of PET/TPU composite nanofiber filter (PET/TPU-CNF)

2.2.1. Preparation of PET and TPU solutions

The PET solution and TPU solution were prepared for PET/TPU nanofiber membrane fabrication. The PET solution at a concentration of 16 wt% was prepared by dissolving PET in a mixture of TFA/DCM (4/1, w/w) and stirring for 6 h. TPU solution at a concentration of 20 wt% was prepared by dissolving TPU in a mixture of DMF/THF (4/1, w/w) and stirring for 6 h.

2.2.2. Fabrication of PET/TPU nanofiber membrane and PET/TPU-CNF

The DXES-1 electrospinning system (Shanghai Oriental Flying Nano-technology Co., Ltd., China) was used for the fabrication of PET/TPU nanofiber membrane and PET/TPU-CNF. The schematic of co-electrospinning was shown in Fig. 1a. Briefly, the PET and TPU homogeneous solutions were separately loaded into two 5 ml glass syringes with metal needles, and the feed rate of both solutions was set as 1 ml/h. The rotating drum collector, which was used to promote the uniform blending of nanofibers during the electrospinning process, was covered with the substrate. A tip-to-collector distance of 24 cm, a rotating speed of the drum collector of 150 r/min, and a high voltage of 15 kV were applied for the electrospinning procedure. The ambient temperature was 25 ± 3 °C, and the humidity was kept at 45 ± 5%.

In particular, the glass syringe filled with TPU solution was wrapped with a heating tape with a temperature controller which was used to control the temperature in real-time. Before the electrospinning started, the temperature of the TPU solution was preheated to 105 °C and this temperature was maintained throughout the electrospinning process, which kept the TPU at a desired viscosity before it was in contact with the substrate. For the fabrication of pure PET nanofiber membrane and pure TPU nanofiber membrane, two 5 ml syringes filled with the corresponding polymer solutions were employed, and other electrospinning parameters were the same as those mentioned earlier.

2.3. Characterization of morphology, adhesion strength and mechanical property

2.3.1. Morphology and structure of the nanofiber membrane

The morphology of the nanofiber membrane was characterized by field-emission scanning electron microscopy (SEM, MERLIN VP Compact). For each type of membrane, three SEM samples with an area of 5 mm² were randomly cut from the whole nanofiber membrane (900 cm²), and three images were taken for each SEM sample. Image J software was employed to analyze the nanofiber diameter. The statistics of the average nanofiber diameters were derived from 9 SEM images which included more than 100 nanofibers. The membrane was immersed in epoxy resin, cured and sliced, and the thickness of the membrane was measured via an optical microscope (Fig. S2). The porosity of the nanofiber membrane was defined as:

$$\text{Porosity}(\%) = 1 - \frac{\rho}{\rho_0} \quad (1)$$

where ρ and ρ_0 are the bulk density of the porous structures and the density of the solid parts, respectively. The value of ρ was obtained by measuring the mass and volume of the nanofiber membrane sample, and ρ_0 was obtained using a Gas Displacement Pycnometry System (Micromeritics, AccuPyc II 1340). The values of ρ_0 for PET nanofiber membrane and PET/TPU nanofiber membrane were 1.37 and 1.3 mg/cm³, respectively.

2.3.2. Evaluation of the adhesion strength between nanofiber membrane and substrate

As shown in Fig. 1b, 90° peeling test was used to evaluate the adhesion strength between the PET/TPU nanofiber membrane and substrate. The PET/TPU-CNF sample was cut into strips of 2 × 6 cm². The substrate and PET/TPU nanofiber membrane were fixed on the stationary platform and the movable clamp of the force gauge (DS2-5 N), respectively. The PET/TPU nanofiber membrane was peeled away from the substrate at a 90° angle with a constant speed of 50 mm/min. The force value was recorded to calculate the adhesion strength of the entire sample. To make the data comparable to previous studies, the force was normalized to the width of the sample.

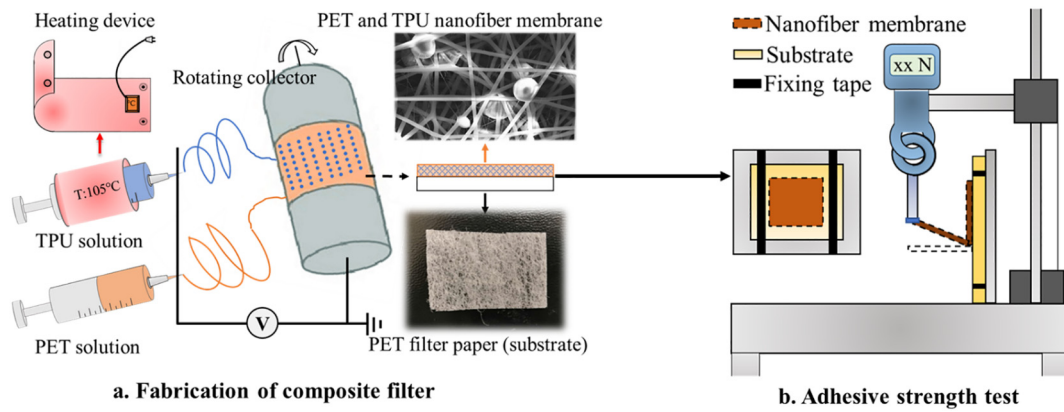


Fig. 1. (a) Schematic of the fabrication procedure of three-dimensional PET/TPU-CNF with beads and fibers structures via co-electrospinning; (b) Schematic of the adhesion strength test for PET/TPU-CNF.

2.3.3. Mechanical property test of the nanofiber membrane

Tensile strength and elongation, which represent the ability of a material to withstand the maximum amount of tensile stress and the ratio between the increased length and initial length at break, respectively, were measured using a tensile tester (XQ-1C, Shanghai New Fiber Instrument Co. Ltd. China) with an extension rate of 10 mm/min and a gauge length of 10 mm. The test membranes were cut into rectangular-shaped samples (5 × 25 mm²). Each type of nanofiber membrane was tested with at least 5 samples to calculate the average value.

2.4. Tests of filtration performances

2.4.1. Quality factor test

The pressure drop was measured by a pressure gauge, and the number based filtration efficiency of the nanofiber composite filters for ambient particles in the laboratory was evaluated via the test bench shown in Fig. 2a. The ambient aerosols were neutralized by a Kr85 neutralizer and then introduced into the filter holder to challenge the nanofiber composite filters. An aerodynamic particle sizer (APS, Model 3321, TSI

Inc., MN, USA) was used to measure the particle concentrations up- and down- stream. The distribution/concentration of ambient aerosols in the laboratory were monitored during the test. The results showed that the ambient aerosols in the laboratory were stable with a total concentration of 3000–4000/cm³ in the size range of 0.5–10 μm (Fig. 2c). The quality factor (Q_f), which reveals the relationship between filtration efficiency and pressure drop, was calculated to determine the PET/TPU-CNF with the optimal fabrication parameters. Q_f was defined as:

$$Q_f = - \frac{\ln(1-\eta)}{\Delta P} \tag{2}$$

where η is the filtration efficiency; ΔP is the pressure drop through the filter media.

2.4.2. Evaluation of the filtration efficiency of the optimal PET/TPU-CNF for nanoscale particles

As shown in Fig. 2b, NaCl solution was aerosolized to generate poly-disperse particles by an atomizer (TSI 3079A), and then the particles were dried by a diffusion dryer. A differential mobility analyzer (DMA,

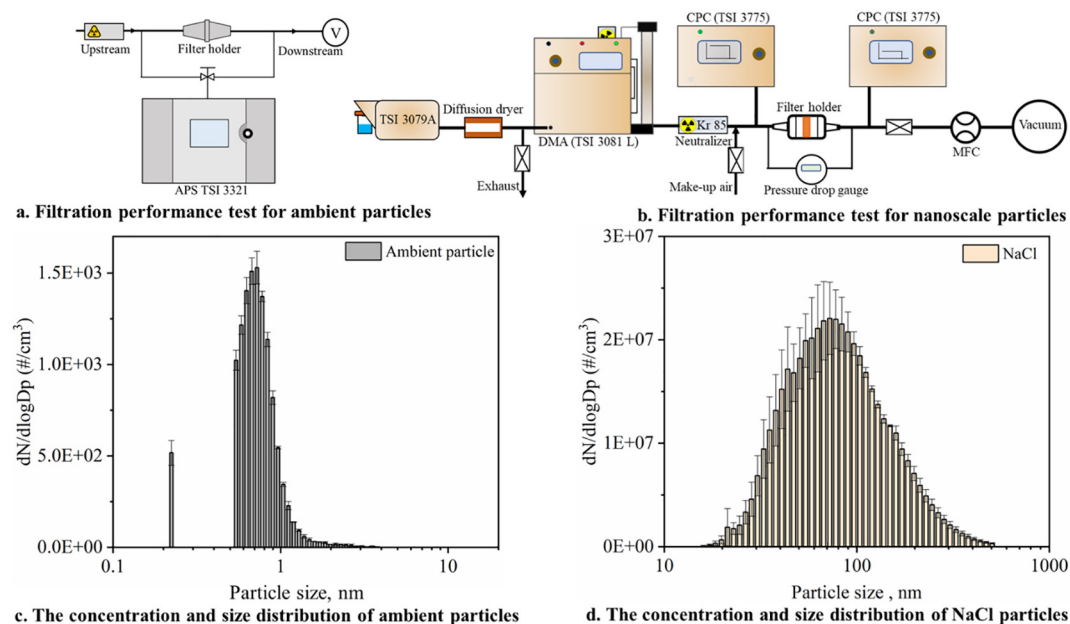


Fig. 2. (a) Experimental setup of filtration test using ambient aerosols in the laboratory; (b) Experimental setup of nanoscale particles filtration test; (c) The size distribution of ambient aerosols in the laboratory during the particle filtration test; (d) The size distribution of nanoscale particles during the particle filtration test.

TSI 3081, USA) was used to select the particles with mobility diameters of 50, 75, 100, 150, 200, 250, 300, 350, 400, 450, and 500 nm from the polydisperse particles. After being neutralized by a neutralizer (Kr-85 source, TSI 3077A, USA), the particles entered the filter chamber. The particle concentrations of upstream (C_{up}) and downstream (C_{down}) were detected by two condensation particle counters (CPC, TSI 3775, USA). The concentration and size distribution of NaCl particles were shown in Fig. 2d. The test velocity was 5.3 cm/s, and the particle filtration efficiency (E) was calculated as follows:

$$E = \left(1 - \frac{C_{up}}{C_{down}}\right) \times 100\% \quad (3)$$

2.4.3. Measurement of the electrostatic potential of PET/TPU nanofibers in nanoscale

The filtration performance of air filters highly depends on the electrostatic property of the fibers. Herein, the electrostatic potentials of PET/TPU nanofibers and pure PET nanofibers were measured by Scanning Kelvin Probe Microscopy (SKPM). The classical Kelvin probe technique and atomic force microscopy (AFM) are combined in this technique, which can increase spatial resolution because of small tip size and precise position control [26]. PET/TPU nanofibers were electrospun on silicon wafers directly, and then the electrostatic potential of a single nanofiber was measured by AFM (Solver Nano, NT-MDT Spectrum Instruments Group, Russia) in SKPM mode.

3. Results and discussions

3.1. Morphology and structure of nanofiber membrane

As shown in Fig. 3b, the fibers and beads co-existed in the pure TPU nanofiber membrane. Some TPU fibers connected the beads and some fibers wrapped the beads on their surfaces; the average diameter of nanofibers and beads were 126 ± 46 and 2028 ± 1021 nm, respectively (Fig. 3b and e). By contrast, the pure PET nanofiber membrane consisted of uniform and randomly oriented fibers with an average diameter of

635 ± 186 nm, and no bead was observed (Fig. 3a and d). As shown in Fig. 3c, the PET/TPU nanofiber membrane presented a three-dimensional structure with beads-on-string. In the PET/TPU nanofiber membrane, the average diameter of beads was 2050 ± 900 nm which was almost the same as the bead size in the pure TPU nanofiber membrane; the average diameter of nanofibers was 395 ± 240 nm (Fig. 3c and f). The smooth and continuous PET nanofibers formed a stable frame, in which the TPU beads were inserted and distributed uniformly in the whole nanofiber membrane. Statistics from the SEM images (Fig. S3) indicated that there were 3748 ± 221 beads per square millimeter. The diameter distributions of the nanofibers and beads in the pure PET nanofiber membrane, pure TPU nanofiber membrane, and PET/TPU nanofiber membrane were shown in Fig. S4.

The electrospun fibers with beads were related to the instability of the polymer solution jet, which was affected by many parameters, such as the applied voltage, ambient humidity, and the conductivity of solution [27–30]. By controlling the mixing amount of ionic liquids, Xing et al. produced the electrospun TPU membrane with beads-on-string morphologies [31]. Herein, all the electrospinning parameters were kept constant while the temperature of TPU solution was set at room temperature and 105 °C. No beads were observed in the TPU nanofiber membrane produced at room temperature (Fig. S1b and c). Thus, it was concluded that the beads-on-string structure of the TPU nanofiber membrane in the present study was caused by the high temperature of the TPU solution. The increased temperature reduced the viscosity of the solution, which led to the entanglement between macromolecular chains to be too weak to resist electrostatic repulsion and further caused the solution jet to break into droplets [32,33]. The rotating collector and traversing spinneret ensured the uniform blending of nanofibers and beads during the electrospinning process.

3.2. Adhesion strength between PET/TPU nanofiber membrane and substrate

With different electrospinning durations, the adhesion strength between the PET/TPU nanofiber membrane and substrate was in the range of 1.01–1.55 N/cm. In comparison, the range of adhesion strength

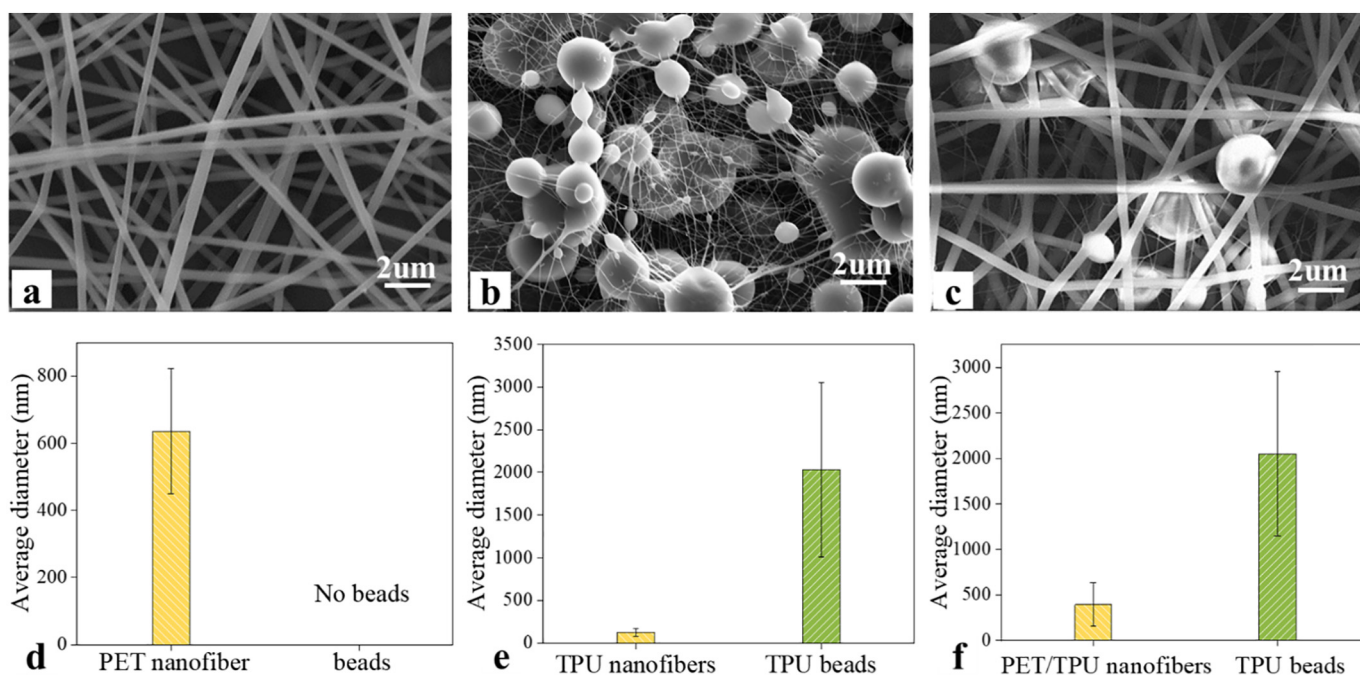


Fig. 3. SEM images of (a) PET nanofiber membrane, (b) TPU nanofiber membrane, (c) PET/TPU nanofiber membrane; the average diameters of fibers and beads in (d) PET nanofiber membrane, (e) TPU nanofiber membrane, (f) PET/TPU nanofiber membrane.

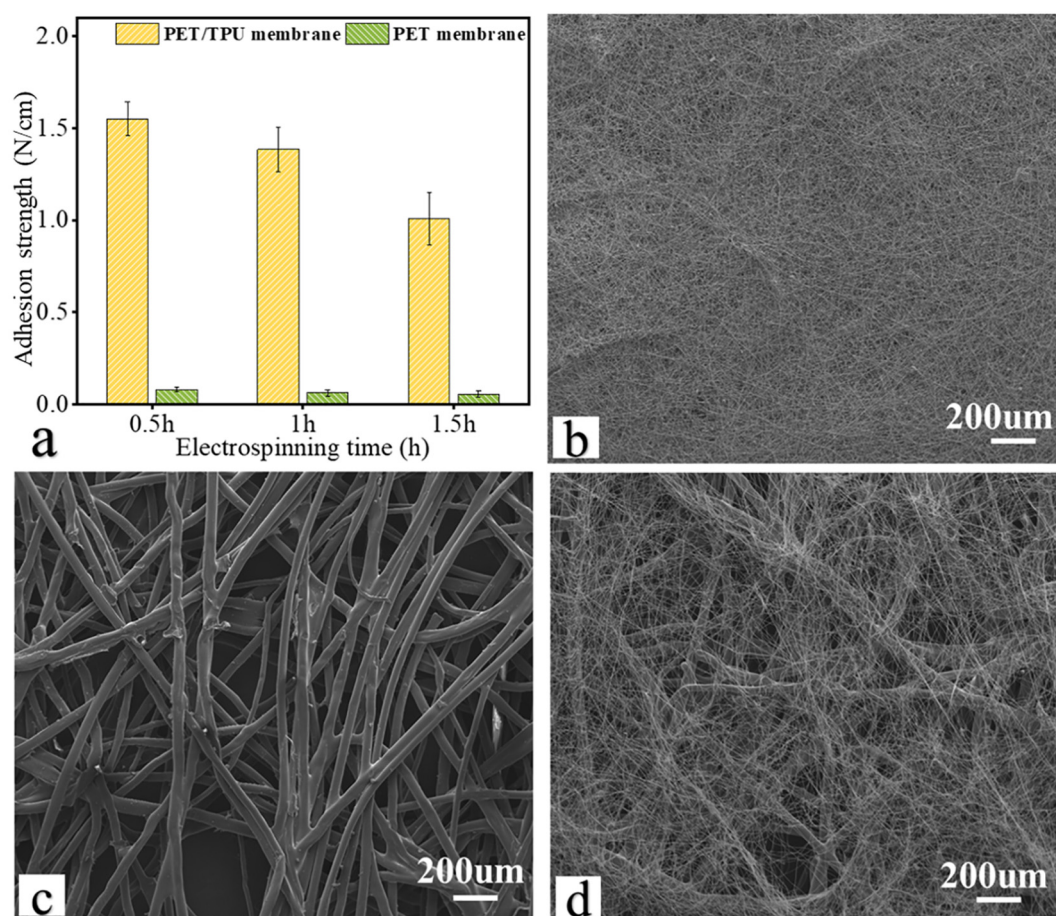


Fig. 4. (a) The adhesion strength between nanofiber membrane and substrate in PET/TPU-CNF and PET-CNF, with different electrospinning durations; SEM images of (b) the surface of PET/TPU-CNF before adhesion strength test, (c) the surface of PET/TPU-CNF with 0.5 h electrospinning duration after adhesion strength test, (d) the surface of PET/TPU-CNF with 1 h electrospinning duration after adhesion strength test.

between the pure PET nanofiber membrane and substrate was 0.057–0.08 N/cm (Fig. 4a). Such a drastic change by more than one order of magnitude indicated that TPU adhesive was the primary reason for the improvement of adhesion strength. In addition to the material adhesive property, TPU nanofibers with smaller fiber diameters had larger contact area with the substrate, which also contributed to the better adhesion of the PET/TPU nanofiber membrane to the substrate [34]. Furthermore, the TPU beads formed numerous bonding points at the interface of the nanofiber membrane and substrate, while the TPU nanofibers cross-linked with PET nanofibers. The adhesion strength between the interfaces of nanofiber layers increased with the decrease of polymer solidification rate [35]. In the present study, the high temperature slowed the solidification rate of TPU polymer, which further enhanced the adhesion strength between the PET/TPU nanofiber membrane and substrate.

The adhesion strength between the PET/TPU nanofiber membrane and substrate decreased with the increase of electrospinning duration (Fig. 4a). The electrospinning duration determined the thickness of the nanofiber membrane, which indicated that increasing the membrane thickness did not further improve the adhesion strength. The PET/TPU nanofiber membrane was spun layer by layer. Only the first several layers linked with the substrate and contributed to the adhesive function. A comparison of Fig. 4b and c indicated that the PET/TPU nanofiber membrane was almost completely removed from the substrate after the adhesion strength test when the electrospinning duration was 0.5 h; the measured adhesion strength was 1.55 N/cm. A breaking interface could be observed between the PET/TPU nanofiber membrane and the substrate. For the PET/TPU nanofiber membranes with the

electrospinning duration of 1 and 1.5 h, the adhesion strengths were 1.38 and 1.01 N/cm, respectively. It was found that the breaking interface was within the nanofiber membrane itself rather than at the interface between the nanofiber membrane and substrate (Fig. 4d). It can be concluded that the adhesion strength between internal layers of the PET/TPU nanofiber membrane was weaker than that between the PET/TPU nanofiber membrane and substrate. Similarly, the pure PET nanofiber membrane could be completely removed from the substrate when the electrospinning duration was 0.5 h. When the electrospinning duration was prolonged to 1 and 1.5 h, the breaking interface was within the pure PET nanofiber membrane rather than at the interface between the nanofiber membrane and substrate. The adhesion strengths between the pure PET nanofiber membrane and the substrate at electrospinning duration of 0.5, 1, 1.5 h were 0.08, 0.063, and 0.057 N/cm, respectively. For the nanofiber membranes with electrospinning durations of 1 and 1.5 h, the measured adhesion strengths were considered as that among the interlayers of nanofiber membrane. Overall, compared to the PET-CNF, significant improvement of adhesion strength was achieved not only at the interface of the PET/TPU nanofiber membrane and substrate, but also among the interlayers of the PET/TPU nanofiber membrane.

As shown in Table 1, the adhesion strengths between the nanofiber membrane and substrate were in the range of 0.045–2.1 N/cm in previous studies [34,36–40]. In particular, the adhesion strengths of membrane coated filter media were in the range of 0.045–0.22 N/cm. For the PET/TPU-CNF fabricated in the present study, the adhesion strength between the nanofiber membrane and substrate was increased up to 1.55 N/cm. The morphology of PET/TPU nanofiber membrane in PET/

Table 1

Comparison of membrane adhesion strengths of the PET/TPU-CNF and other nanofiber composite materials (the force was normalized to the width of the sample).

Ref.	Adhesion strength (N/cm)	Nanofiber membrane	Substrate	Assisting adhesive or reagent	Composite method	Application field
[36]	0.045	Nylon 66/PVA ^a	PET ^b fabric	None	Hot press	Air filtration, protective clothing
[37]	1.7	PVDFhfp ^c	Cured PDMS ^d /TEGO21002	Uncured PDMS/TEGO21002 ^e	Hot drying	Medical devices, textiles
[38]	0.1	PVA	ES ^f nonwoven	None	Hot press	Air filtration
[34]	~2.1	PVDF-co-CTFE ^g	PP ^h membrane	None	Hot press	Battery separators
[39]	0.51	Silk fibroin	Cotton gauze	None	Post-treatment by helium plasma	Wound dressings
[40]	0.22	PEO ⁱ	PEG ^j -grafted SEBS ^k film	Glutaraldehyde	Cross-linking reaction	Filtration, textile
Present study	1.55	PET/TPU ^m	PET nonwoven	None	Co-electrospun with hot TPU	Air filtration

- ^a PVA – Polyvinylalcohol.
- ^b PET – Polyester.
- ^c PVDFhfp - Poly (vinylidene fluoride-co-hexafluoropropylene).
- ^d PDMS – Polydimethylsiloxane.
- ^e TEGO21002 - epoxy siloxane TEGOMER® XP 21002.
- ^f ES - Ethylene-propylene side-by-side.
- ^g PVDF-co-CTFE - Polyvinylidene fluoride-co-chlorotrifluoroethylene.
- ^h PP – polypropylene.
- ⁱ PEO - Poly (ethylene oxide).
- ^j PEG - Poly(ethylene glycol).
- ^k SEBS - styrene-b-(ethylene-co-butylene)-b-styrene elastomer.
- ^m TPU - Thermoplastic polyurethane.

TPU-CNF was maintained in the present study, and almost no extra pressure drop was added during the composite process compared with PET-CNF (Fig. 6b). By contrast, hot pressing, the commonly used technique to improve the adhesion strength of membrane coated air filter, would damage the morphology of nanofibers (Fig. S5), which decreased the porosity and increased the pressure drop of nanofiber membranes [41].

3.3. Mechanical properties

The tensile strength and elongation are related to the abilities of materials to resist tearing and shape changes [41,42], and thus these two parameters of nanofibrous membranes are crucial for the practical applications. Many researchers focus on the improvement of mechanical properties of PET nanofiber membranes by electrospinning with

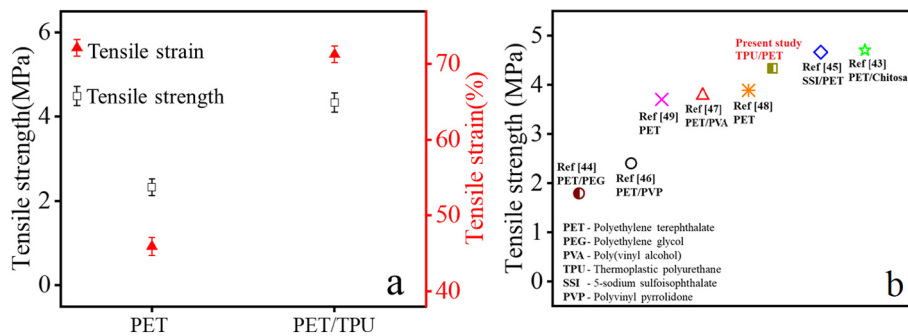


Fig. 5. (a) The tensile strength and tensile strain (elongation) of the pure PET and PET/TPU nanofiber membrane; (b) comparison of the tensile strength with those in other studies.

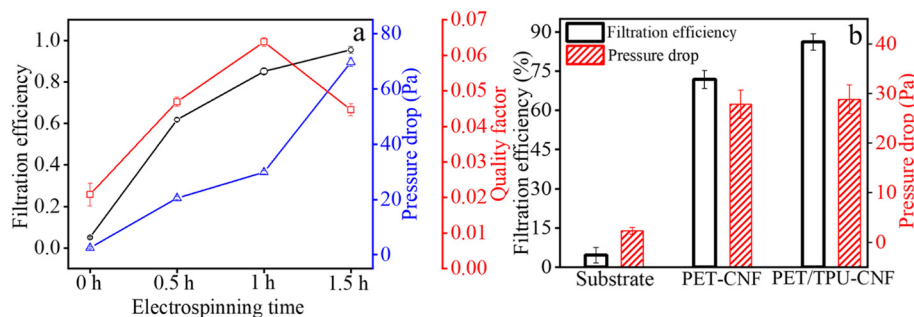


Fig. 6. (a) The filtration efficiency, Q_f , and the pressure drop of PET/TPU-CNF with different electrospinning durations in the ambient particle filtration test; (b) filtration efficiency and pressure drop of the substrate, PET-CNF, and PET/TPU-CNF (with the electrospinning duration of 1 h) for the ambient particles in the laboratory.

Table 2

Properties (average diameter, porosity and thickness) of nanofiber membranes.

Type of nanofiber membrane	Average diameter (nm)		Thickness (μm)	Porosity (%)
	Fibers	Beads		
PET	635	–	27	88.29
PET/TPU	395	2050	35	94.3

mixed polymer solutions, such as chitosan, poly(vinyl alcohol) (PVA), dimethyl 5-sodium sulfoisophthalate (SSI), poly(vinyl pyrrolidone) (PVP), and polyethylene glycol (PEG). The tensile strength and elongation of these PET nanofiber-based membranes were in the range of 1.91–4.7 MPa and 12–243%, respectively [43–47]. It has also been reported that the tensile strength of the PET nanofiber membrane could be improved by heat treatment or adjusting the polymer concentration [48,49]. In this study, the PET/TPU nanofiber membrane with an electrospinning duration of 1 h had a tensile strength of 4.33 MPa and

an elongation of 71.28%, while the tensile strength and elongation of the pure PET nanofiber membrane with the same electrospinning duration were 2.33 MPa and 45.94%, respectively (Fig. 5a). Compared with the PET-based nanofiber membranes of previous studies, the tensile strength of the PET/TPU nanofiber membrane in the present study was among the better ones (Fig. 5b).

The higher tensile strength and elongation of the PET/TPU nanofiber membrane were attributed to the presence of TPU and the beads-on-string structure of the PET/TPU nanofiber membrane. First, TPU possesses the characteristics of superior ductility, high elongation, and great toughness [50]. Thereby, it can enhance the tensile strength and elongation of the entire composite material when it is added to fibrous products [51]. Moreover, an effective approach to increase the tensile strength of the nanofiber membrane is to enhance the binding strength between the fibers at their junction points throughout the fiber membrane [52,53]. Herein, the TPU nanofibers and beads were distributed throughout the entire volume of the PET/TPU nanofiber membrane, which significantly increased the binding strength between nanofibers.

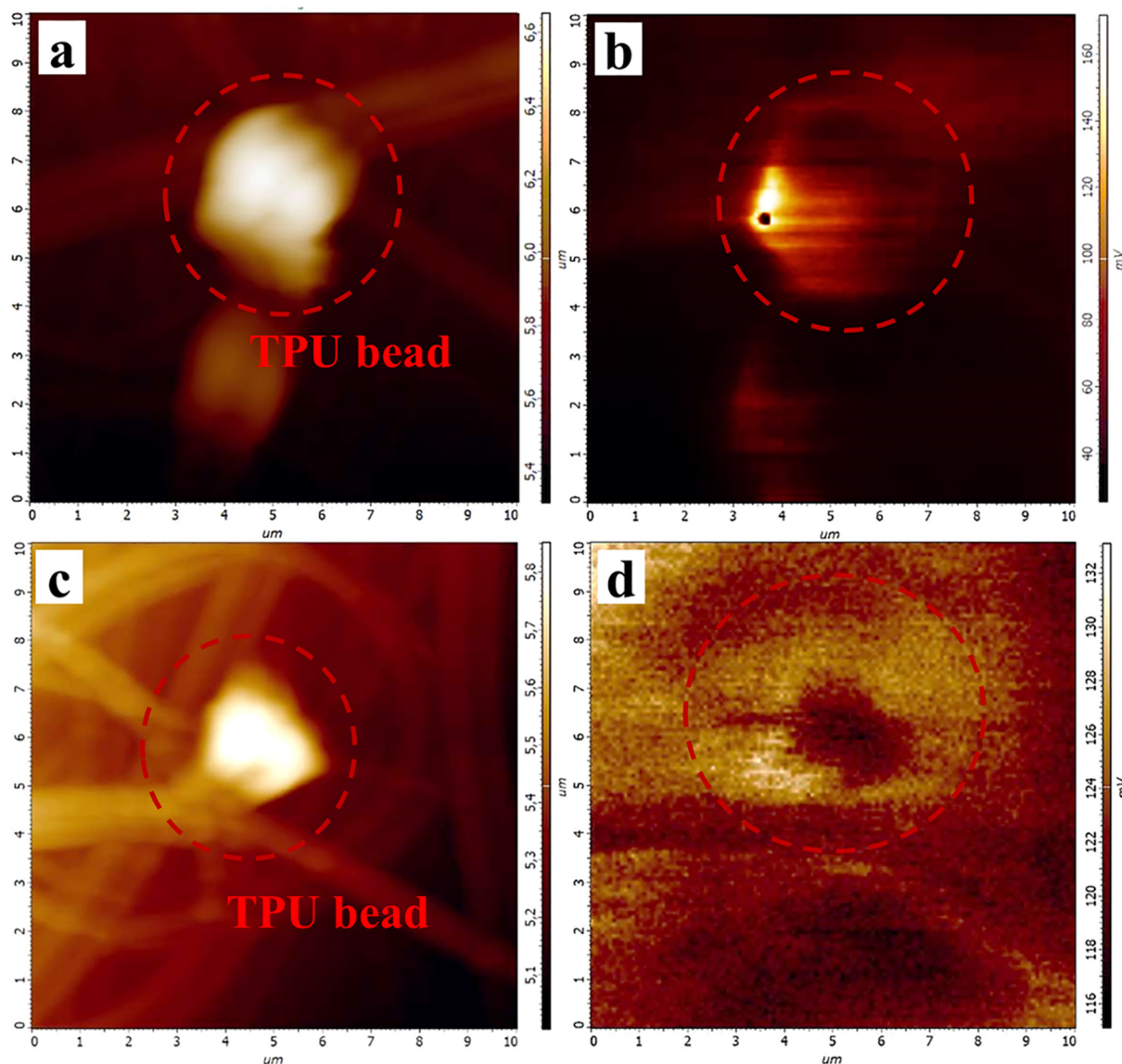


Fig. 7. (a, c) AFM topographies of the PET/TPU nanofibers with beads; (b, d) corresponding SKPM potential images.

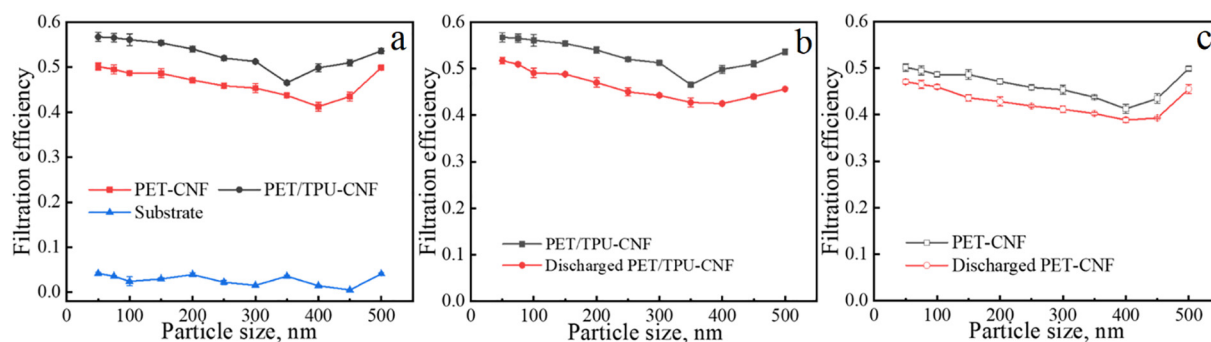


Fig. 8. (a) Filtration efficiency of the substrate, PET-CNF, and PET/TPU-CNF for nanoscale particles; (b) the filtration efficiency comparison of the untreated PET/TPU-CNF and the discharged PET/TPU-CNF; (c) the filtration efficiency comparison of the untreated PET-CNF and the discharged PET-CNF.

3.4. Filtration performance

3.4.1. Assessment of filtration efficiency and Q_f for the ambient particles in the laboratory

Compared with the substrate, the filtration efficiency of PET/TPU-CNF for the ambient particles in the laboratory increased from 5.0% to 61.8%, when the electrospinning duration of PET/TPU nanofiber membrane was 0.5 h. It is well known that nanofibers are characterized by a very large surface area to volume ratio, which significantly increased the probability of the deposition of aerosol particles on the fiber surface and thereby improves the filter efficiency [54,55]. With the electrospinning duration increasing from 0.5 to 1.5 h, the filtration efficiency of PET/TPU-CNF for ambient particles increased from 61.8% to 95.6% while the pressure drop increased from 20.5 to 69.7 Pa. As shown in Fig. 6a, the Q_f values of PET/TPU-CNF with the electrospinning duration of 0, 0.5, 1, and 1.5 h were 0.020, 0.046, 0.064, and 0.045 Pa⁻¹, respectively. The optimal Q_f value of PET/TPU-CNF was observed at the electrospinning duration of 1 h. The pressure drop and filtration efficiency data of the substrate, PET-CNF, and PET/TPU-CNF (with electrospinning duration of 1 h) for the ambient particles in the laboratory were shown in Fig. 6b.

3.4.2. Evaluation of the filtration efficiency for nanoscale particles

The PET/TPU-CNF with the maximum Q_f value (0.064 Pa⁻¹) was used for the filtration test of monodisperse particles in the range of 50–500 nm, and the results were compared to PET-CNF. Similar to the trend observed in previous studies [56], the composite filters with nanofibers showed enhanced filtration efficiency and reduced MPPS (most penetrating particle size) compared to conventional microfiber filters (Fig. 8a). The MPPS of PET/TPU-CNF and PET-CNF were 350 and 400 nm, respectively. For the substrate, the MPPS was not observed in the size range of the test particles.

Compared with PET-CNF, the PET/TPU-CNF with the same electrospinning duration of 1 h showed higher filtration efficiency and smaller MPPS, which was caused by the differences between PET/TPU nanofibers and pure PET nanofibers in the structure and electrostatic property.

In terms of the membrane structure, the porosity and fiber diameter might be the main influencing factors. On one hand, the incorporation of TPU beads into PET nanofibers increased the spacing between nanofibers, which indicated that the PET/TPU nanofiber membrane was thicker than the pure PET nanofiber membrane. As measured, the thicknesses of PET/TPU and pure PET nanofiber membranes with the same electrospinning duration were 35 and 27 μm , respectively. For the samples of PET/TPU and pure PET nanofiber membrane with a same area of 8×8 cm, the thicker thickness indicated a bigger volume and a smaller bulk density (ρ). According to Eq. (1), the porosity increased with the decreasing of bulk density. As shown in Table 2, the porosity of PET/TPU

and pure PET nanofiber membrane were 94.30% and 88.29%, respectively. The higher porosity indicated more fibers were exposed to the incoming airflow, thus resulting in a higher filtration efficiency. On the other hand, it is well known that the MPPS of a fabric filter decreases with the decreasing of fiber diameter [57,58]. In the present study, the average fiber diameter of the PET/TPU nanofiber membrane was 395 ± 240 nm, which was much smaller than that of the pure PET nanofiber membrane (635 ± 186 nm).

In the aspect of electrostatic property, the stronger electrostatic effect could contribute to higher filtration efficiency and smaller MPPS [59]. As shown in Fig. 7b and d, the measured electrostatic potential around TPU beads in PET/TPU nanofibers was 120–165 mV, which was much higher than other areas (30–80 mV). More measurement results of surface potential were shown in Fig. S6. The higher electrostatic potential of TPU may be caused by its higher charge storage ability. The ability of a material to store charges increases as the dielectric constant increases, and the dielectric constants of PET and TPU are 2.8–5 and 7, respectively [60,61].

In order to identify the contribution of the electrostatic effects, the PET/TPU-CNF and PET-CNF were discharged by isopropanol (IPA) saturated vapor for 24 h in a chamber and then dried in ambient environment for at least 30 min. This IPA discharging method was based on ISO 16890-4:2016 [62]. The filtration efficiency comparison between the untreated media (PET/TPU-CNF and PET-CNF) and the discharged media (discharged PET/TPU-CNF and discharged PET-CNF) was shown in Fig. 8b and c. The filtration efficiency degradation was observed in the discharged PET/TPU-CNF and the discharged PET-CNF, which indicated that the electrostatic effects existed not only in the PET/TPU-CNF but also in the PET-CNF. Actually, in our previous study, it was revealed that both surface charges and volume charges were formed during electrospinning [26]. The results of the present study further confirmed our previous conclusion. In addition, the average filtration efficiencies of the PET/TPU-CNF and the PET-CNF decreased by $6.5 \pm 0.58\%$ and $2.5 \pm 0.60\%$ after discharging treatment, respectively. The results demonstrated that the electrostatic filtration mechanism played a stronger role for the PET/TPU fibers than for the pure PET fibers. The stronger electrostatic contribution on the PET/TPU fibers might be induced by inserting TPU beads and fibers, which were consistent with the results of electrostatic potential test.

4. Conclusions

In summary, three-dimensional PET/TPU composite nanofiber filters (PET/TPU-CNF) with beads-on-string structure have been successfully fabricated by one step co-electrospinning. Thanks to the temperature control of the TPU solution, the TPU beads and thin nanofibers were stuck on the substrate and intertwined with PET nanofibers, which contributed to a strong adhesion strength between the PET/TPU nanofiber

membrane and substrate. The PET/TPU-CNF showed high filtration efficiency for ambient particles and nanoscale particles. Compared with the pure PET nanofiber composite filter (PET-CNF), the PET/TPU-CNF had greater surface potential, which contributed to the higher filtration efficiency and smaller most penetrating particle size. Furthermore, the embedded TPU beads and nanofibers also significantly improved the tensile strength of the PET/TPU nanofiber membrane. Overall, the one-step co-electrospinning has been successfully performed to prepare the nanofiber-based air filter that has enhanced membrane adhesion strength, improved membrane tensile strength, unbroken nanofiber structure, and satisfactory filtration efficiency. This work provided a potential strategy for the further advancement of the functional composite nanofiber media for various applications, including air/water filtration, wound dressings, and battery separators.

Declaration of competing interest

The authors declare that they have no known competing financial interests or personal relationships that could have appeared to influence the work reported in this paper.

Acknowledgements

The work was partially supported by Center for Filtration Research at University of Minnesota. We thank the support of National Science and Technology Major Project of China (Award ID: 2017YFC0211801; 2016YFC0801704; 2016YFC0203701; 2016YFC0801605; 2019JH2/10100004). The authors also thank the financial aid from the project of China Scholarship Council, China.

Appendix A. Supplementary data

Supplementary data to this article can be found online at <https://doi.org/10.1016/j.powtec.2021.04.020>.

References

- [1] Q.N. Wang, Y.Y. Bai, J.F. Xie, Q.R. Jiang, Y.P. Qiu, Synthesis and filtration properties of polyimide nanofiber membrane/carbon woven fabric sandwiched hot gas filters for removal of PM 2.5 particles, *Powder Technol.* 292 (2016) 54–63.
- [2] M. Hu, L.H. Yin, N. Low, D.H. Ji, Y.S. Liu, J.F. Yao, Z.X. Zhong, W.H. Xing, Zeolitic-imidazolate-framework filled hierarchical porous nanofiber membrane for air cleaning, *J. Membr. Sci.* 594 (2020) 117467.
- [3] C. Liu, P.C. Hsu, H.W. Lee, M. Ye, G.Y. Zheng, N. Liu, W.Y. Li, Y. Cui, Transparent air filter for high-efficiency PM_{2.5} capture, *Nat. Commun.* 6205 (2015) 1–9.
- [4] J. Wang, S.C. Kim, D.Y. Pui, Investigation of the figure of merit for filters with a single nanofiber layer on a substrate, *J. Aerosol Sci.* 4 (2008) 323–334.
- [5] T.M. Bucher, H.V. Tafreshi, G.C. Tepper, Modeling performance of thin fibrous coatings with orthogonally layered nanofibers for improved aerosol filtration, *Powder Technol.* 249 (2013) 43–53.
- [6] R. Jalili, M. Morshed, S.A.H. Ravandi, Fundamental parameters affecting electrospinning of PAN nanofibers as uniaxially aligned fibers, *J. Appl. Polym. Sci.* 101 (2006) 4350–4357.
- [7] S.S. Choi, Y.S. Lee, C.W. Joo, S.G. Lee, J.K. Park, K.S. Han, Electrospun PVDF nanofiber web as polymer electrolyte or separator, *Electrochim. Acta* 50 (2004) 339–343.
- [8] H. Zhu, S. Qiu, W. Jiang, D. Wu, C. Zhang, Evaluation of electrospun polyvinyl chloride/polystyrene fibers as sorbent materials for oil spill cleanup, *Environ. Sci. Technol.* 45 (2011) 4527–4531.
- [9] C. Huang, S. Chen, D.H. Reneker, C. Lai, H. Hou, High-strength mats from electrospun poly (p-phenylene biphenyltetracarboximide) nanofibers, *Adv. Mater.* 18 (5) (2006) 668–671.
- [10] Y.S. Wang, S.M. Li, S.T. Hsiao, W.H. Liao, P.H. Chen, S.Y. Yang, H.W. Tien, C.C.M. Ma, C.C. Hu, Integration of tailored reduced graphene oxide nanosheets and electrospun polyamide-66 nanofibers for a flexible supercapacitor with high-volume-and high-area-specific capacitance, *Carbon* 73 (2014) 87–98.
- [11] W.W.F. Leung, C.H. Hung, P.T. Yuen, Effect of face velocity, nanofiber packing density and thickness on filtration performance of filters with nanofibers coated on a substrate, *Sep. Purif. Technol.* 71 (2010) 30–37.
- [12] B. Liu, S. Zhang, X. Wang, J. Yu, B. Ding, Efficient and reusable polyamide-56 nanofiber/nets membrane with bimodal structures for air filtration, *J. Colloid Interface Sci.* 457 (2015) 203–211.
- [13] L.C. Ma, N. Li, G.S. Wu, G.J. Song, X.R. Li, P. Han, G. Wang, Y.D. Huang, Interfacial enhancement of carbon fiber composites by growing TiO₂ nanowires onto amine-based functionalized carbon fiber surface in supercritical water, *Appl. Surf. Sci.* 433 (2018) 560–567.
- [14] N. Zheng, Y.D. Huang, W.F. Sun, X.S. Du, H.Y. Liu, S. Moody, J.F. Gao, Y.W. Mai, In-situ pull-off of ZnO nanowire from carbon fiber and improvement of interlaminar toughness of hierarchical ZnO nanowire/carbon fiber hybrid composite laminates, *Carbon* 110 (2016) 69–78.
- [15] Q. Liao, M. Mohr, X. Zhang, Z. Zhang, Y. Zhang, H.J. Fecht, Carbon fiber-ZnO nanowire hybrid structures for flexible and adaptable strain sensors, *Nanoscale* 5 (2013) 12350–12355.
- [16] L. Li, L.M. Shang, Y.X. Li, C.F. Yang, Three-layer composite filter media containing electrospun polyimide nanofibers for the removal of fine particles, *Fibers Polym.* 18 (4) (2017) 749–757.
- [17] A. Wang, R. Fan, X. Zhou, S. Hao, X. Zheng, Y. Yang, Hot-pressing method to prepare imidazole-based zn(ii) metal-organic complexes coatings for highly efficient air filtration, *ACS Appl. Mater. Interfaces* 11 (2018) 9744–9755.
- [18] K.J. Buschow, R.W. Cahn, M.C. Flemings, B. Ilschner, E.J. Kramer, S. Mahajan, Encyclopedia of materials, *Sci. Technol.* 1 (2001) 11.
- [19] M. Drawert, E. Griebisch, W. Imoehl, Polyamide Melt Adhesives, U.S. Patent No. 4,150,002. 17 Apr. 1979.
- [20] C. Ochoa-Putman, U.K. Vaidya, Mechanisms of interfacial adhesion in metal-polymer composites—effect of chemical treatment, *Compos. A: Appl. Sci. Manuf.* 42 (2011) 906–915.
- [21] C. Ons, S. Boufi, Cellulose nanofibrils/polyvinyl acetate nanocomposite adhesives with improved mechanical properties, *Carbohydr. Polym.* 156 (2017) 64–70.
- [22] P. Gatenholm, H. Bertilsson, A. Mathiasson, The effect of chemical composition of interphase on dispersion of cellulose fibers in polymers. I. PVC-coated cellulose in polystyrene, *J. Appl. Polym. Sci.* 49 (1993) 197–208.
- [23] Y.H. Guo, W.D. He, J.X. Liu, Electrospinning polyethylene terephthalate/SiO₂ nanofiber composite needle felt for enhanced filtration performance, *J. Appl. Polym. Sci.* 137 (2020) 48282.
- [24] H. Na, Y. Zhao, C. Zhao, X. Yuan, Effect of hot-press on electrospun poly (vinylidene fluoride) membranes, *Polym. Eng. Sci.* 48 (2008) 934–940.
- [25] H. Na, Y. Zhao, X. Liu, C. Zhao, X. Yuan, Structure and properties of electrospun poly (vinylidene fluoride)/polycarbonate membranes after hot-press, *J. Appl. Polym. Sci.* 122 (2011) 774–781.
- [26] H.C. Gao, W.D. He, Y.B. Zhao, D.M. Opris, G.B. Xu, J. Wang, Electret mechanisms and kinetics of electrospun nanofiber membranes and lifetime in filtration applications in comparison with corona-charged membranes, *J. Membr. Sci.* 600 (2020) 117879.
- [27] A.L. Yarin, *Free Liquid Jets and Films: Hydrodynamics and Rheology*, Wiley, New York, 1993.
- [28] K.H. Lee, H.Y. Kim, H.J. Bang, Y.H. Jung, S.G. Lee, The change of bead morphology formed on electrospun polystyrene fibers, *Polymer* 14 (2003) 4029–4034.
- [29] Y.Y. Kuo, F.C. Bruno, J. Wang, Filtration performance against nanoparticles by electrospun nylon-6 media containing ultrathin nanofibers, *Aerosol Sci. Technol.* 48 (2013) 1332–1344.
- [30] T. Uyar, F. Besenbacher, Electrospinning of uniform polystyrene fibers: the effect of solvent conductivity, *Polymer* 24 (2008) 5336–5343.
- [31] C.Y. Xing, J.P. Guan, Z.L. Chen, Y. Zhu, B.W. Zhang, Y.J. Li, J.Y. Li, Novel multifunctional nanofibers based on thermoplastic polyurethane and ionic liquid: towards antibacterial, anti-electrostatic and hydrophilic nonwovens by electrospinning, *Nanotechnology* 26 (2015) 105704.
- [32] Y.W. Cheng, H.A. Lu, Y.C. Wang, A. Thierry, B. Lotz, C. Wang, Syndiotactic polystyrene nanofibers obtained from high-temperature solution electrospinning process, *Macromolecules* 43 (2010) 2371–2376.
- [33] H. Fong, I. Chun, D.H. Reneker, Beaded nanofibers formed during electrospinning, *Polymer* 40 (1999) 4585–4592.
- [34] M. Alcoutlabi, H. Lee, J.V. Watson, X. Zhang, Preparation and properties of nanofiber-coated composite membranes as battery separators via electrospinning, *J. Mater. Sci.* 48 (2013) 2690–2700.
- [35] N.D.N. Affandi, F. Fadil, M.I. Misnon, Preliminary study on the adhesion strength of electrospun bi-layer membranes by 180° peel test, *Fibers Polym.* 20 (2019) 1317–1322.
- [36] G. Amini, A.A. Gharehaghaji, Improving adhesion of electrospun nanofiber mats to supporting substrate by using adhesive bonding, *Int. J. Adhes. Adhes.* 86 (2018) 40–44.
- [37] M. Brunelli, S. Alther, R.M. Rossi, S.J. Ferguson, M. Rottmar, G. Fortunato, Nanofiber membranes as biomimetic and mechanically stable surface coatings, *Mater. Sci. Eng. C* 108 (2020) 110417.
- [38] C.C. Zhao, Y. Lu, Z.J. Pan, Adhesion and protective properties of electrospun PVA/ES composites obtained by using spiral disk spinnerets, *Text. Res. J.* 14 (2017) 1685–1695.
- [39] R. Nawalalke, Q. Shi, N. Vitthuli, M.A. Bourham, X.W. Zhang, M.G. McCord, Novel atmospheric plasma enhanced silk fibroin nanofiber/gauze composite wound dressings, *J. Fiber Bioeng. Inform.* 3 (2012) 227–242.
- [40] Q. Shi, Q.F. Fan, X.D. Xu, W. Ye, J.W. Hou, S.C. Wong, J.H. Yin, Effect of surface interactions on adhesion of electrospun meshes on substrates, *Langmuir* 45 (2014) 13549–13555.
- [41] Y. Liao, R. Wang, M. Tian, C. Qiu, A.G. Fane, Fabrication of polyvinylidene fluoride (PVDF) nanofiber membranes by electro-spinning for direct contact membrane distillation, *J. Membr. Sci.* 425 (2013) 30–39.
- [42] P. Bajpai, *Biermann's Handbook of Pulp and Paper*, Third edition Elsevier, 2018 35–63.
- [43] J.A. Lopes-da-Silva, V. Beatriz, D. Ivonne Delgadillo, Preparation and characterization of electrospun mats made of PET/chitosan hybrid nanofibers, *J. Nanosci. Nanotechnol.* 6 (2009) 3798–3804.

- [44] L.N. Wang, Z.X. Chang, W.T. Liu, X.L. Xia, S.Q. He, H. Liu, C.S. Zhu, Electrospun PET/PEG fibrous membrane with enhanced mechanical properties and hydrophilicity for filtration applications, *Arab. J. Sci. Eng.* 40 (2015) 2889–2895.
- [45] P. Chegoonian, S.A.H. Ravandi, M. Feiz, S. Mallakpour, Preparation of hydrophilic dimethyl 5-sodium sulfoisophthalate/poly (ethylene terephthalate) nanofiber composite membranes for improving antifouling properties, *J. Appl. Polym. Sci.* 8 (2017) 1–8.
- [46] S.S. Shahrabi, J. Barzin, P. Shokrollahi, Blood cell separation by novel PET/PVP blend electrospun membranes, *Polym. Test.* 66 (2018) 94–104.
- [47] G.H. Li, Y.M. Zhao, M.Q. Lv, Y. Shi, D. Cao, Super hydrophilic poly (ethylene terephthalate)(PET)/poly (vinyl alcohol)(PVA) composite fibrous mats with improved mechanical properties prepared via electrospinning process, *Colloids Surf. A Physicochem. Eng. Asp.* 436 (2013) 417–424.
- [48] H. Mahdavi, M. Moslehi, A new thin film composite nanofiltration membrane based on PET nanofiber support and polyamide top layer: preparation and characterization, *J. Polym. Res.* 12 (2016) 257.
- [49] B. Veleirinho, M.F. Rei, J.A. Lopes-DA-Silva, Solvent and concentration effects on the properties of electrospun poly (ethylene terephthalate) nanofiber mats, *J. Polym. Sci. B Polym. Phys.* 5 (2008) 460–471.
- [50] D. Alhazov, A. Gradys, P. Sajkiewicz, A. Arinstein, E. Zussman, Thermo-mechanical behavior of electrospun thermoplastic polyurethane nanofibers, *Eur. Polym. J.* 49 (2013) 3851–3856.
- [51] S.H. Jiang, G.G. Duan, E. Zussman, A. Greiner, S. Agarwal, Highly flexible and tough concentric triaxial polystyrene fibers, *ACS Appl. Mater. Interfaces* 6 (2014) 5918–5923.
- [52] K. Yoon, B.S. Hsiao, B. Chu, Formation of functional polyethersulfone electrospun membrane for water purification by mixed solvent and oxidation processes, *Polymer* 50 (2009) 2893–2899.
- [53] L. Huang, S.S. Manickam, J.R. McCutcheon, Increasing strength of electrospun nanofiber membranes for water filtration using solvent vapor, *J. Membr. Sci.* 436 (2013) 213–220.
- [54] Z.M. Huang, Y.Z. Zhang, M. Kotaki, S. Ramakrishna, A review on polymer nanofibers by electrospinning and their applications in nanocomposites, *Compos. Sci. Technol.* 63 (2003) 2223–2253.
- [55] H.R. Park, Y.O. Park, Filtration properties of electrospun ultrafine fiber webs, *Korean J. Chem. Eng.* 22 (2005) 165–172.
- [56] A. Podgórski, Estimation of the upper limit of aerosol nanoparticles penetration through inhomogeneous fibrous filters, *J. Nanopart. Res.* 11 (2009) 197–207.
- [57] K.W. Lee, B.Y.H. Liu, On the minimum efficiency and most penetrating particle size for fibrous filters, *J. Air Pollut. Control Assoc.* 30 (1980) 377–381.
- [58] K.M. Yun, A.B. Suryamas, F. Iskandar, L. Bao, H. Niinuma, K. Okuyama, Morphology optimization of polymer nanofiber for applications in aerosol particle filtration, *Sep. Purif. Technol.* 75 (2010) 340–345.
- [59] D.Q. Chang, S.C. Chen, A.R. Fox, A.S. Viner, D.Y. Pui, Penetration of sub-50 nm nanoparticles through electret HVAC filters used in residence, *Aerosol Sci. Technol.* 49 (2015) 966–976.
- [60] A.K. Barick, D.K. Tripathy, Effect of nanofiber on material properties of vapor-grown carbon nanofiber reinforced thermoplastic polyurethane (TPU/CNF) nanocomposites prepared by melt compounding, *Compos. A: Appl. Sci. Manuf.* 10 (2010) 1471–1482.
- [61] F. Carpi, D.D. Rossi, R. Kornbluh, R.E. Pelrine, P. Sommer-Larsen, Dielectric Elastomers as Electromechanical Transducers: Fundamentals, Materials, Devices, Models and Applications of an Emerging Electroactive Polymer Technology, Elsevier, 2011.
- [62] ISO 16890–16894, Air Filters for General Ventilation - Part 4: Conditioning Method to Determine the Minimum Fractional Test Efficiency, International Organization for Standardization, Geneva, Switzerland, 2016.